Life Sciences 232 (2019) 116591

Contents lists available at ScienceDirect

Life Sciences

journal homepage: www.elsevier.com/locate/lifescie

Calreticulin stabilizes F-actin by acetylating actin and protects microvascular endothelial cells against microwave radiation

Xiaoreng Wang, Tianqi Tao, Dandan Song, Huimin Mao, Mi Liu, Jianli Wang, Xiuhua Liu*

Department of Pathophysiology, Chinese PLA General Hospital, Beijing, China

ARTICLE INFO

Keywords:
Calreticulin
Acetylation
F-actin
Microwave radiation

ABSTRACT

Aims: Calreticulin (CRT) is a multifunctional protein that protects endothelial cells by alleviating actin cytoskeleton injury, but the underlying mechanism remains unclear. CRT was recently identified as a novel acyltransferase; acetylation at the N-terminus of actin monomers strengthens actin polymerization. This study was undertaken to determine whether CRT protects human microvascular endothelial cells (HMECs) against microwave radiation through actin acetylation.

Materials and methods: We prepared a eukaryotic-derived recombinant CRT and incubated the HMECs with it prior to microwave exposure. We then assessed cell injury and endothelial function, detected actin polymerization and acetylation after HMECs exposure to S-band high-power microwaves. Coimmunoprecipitation, pull-down, and ex vitro acetylation reaction were performed to determine whether actin is a novel substrate of CRT acyltransferase. Finally, we employed the mutant experiments to demonstrate the acetylation sites contributing to CRT acetyltransferase activity.

Key findings: Microwave radiation induced severe cell injury and endothelial contact dysfunction, reduced the polymerization of actin filaments, and destroyed the actin arrangement, ultimately reducing acetylated actin expression. CRT treatment upregulated actin acetylation levels, promoted polymerization, and facilitated thicker and longer F-actin stress fibre formation. Pre-incubation with CRT rescued microwave-induced cell injury, decreased actin acetylation, and rendered the actin cytoskeleton radiation-retardant. The level of acetyl-actin was positively correlated with actin polymerization. Actin was identified as a novel substrate of CRT, being acetylated mainly through the CRT P-domain at lys-206 and -207.

Significance: This work provides a better understanding of the underlying mechanism of CRT-induced cytoprotection, and suggests a novel therapeutic target for microwave radiation-related diseases with endothelial dysfunction.

1. Introduction

With the extensive use of wireless technology in daily life, the hazard of human exposure to electromagnetic radiation from microwaves pervading the environment has been increasingly recognised as a severe “electro-pollution” [1]. The microwave can be divided into several bands according to its frequency. The S-band (2–4 GHz) microwave, which is mainly produced by signal relay, satellite communications, radar, wireless routers, mobile phones, and bluetooth equipment, is the most widely utilized in daily life. S-band or near S-band microwave radiation may damage several systems and organs, including the reproductive system [2,3], nervous system [4,5], liver [6], and cardiovascular system. In particular, the microcirculature throughout the body is sensitive to microwaves [7]. A certain density of S-band microwave radiation leads to capillary malformation, decreased blood flow [8], and increased microvascular permeability [9]. Endothelial cells, which line the inner surface of microvascular blood vessels, form a selective barrier between blood and tissues to maintain homeostasis. Microvascular endothelial cell injury induces endothelial dysfunction and results in physiological disorders. Attenuation of microvascular endothelial cell injury might be an effective strategy to prevent the microwave radiation hazard.

The integrity and stabilization of actin cytoskeleton is critical for endothelial cell resistance to certain types of injury, by connecting transmembrane proteins in tight and adhesion junctions, and by maintaining cellular morphology, movement, growth, and differentiation [10]. Polymerization of the monomer globular actin (G-actin) and depolymerization of the fibrous actin (F-actin) dynamic balance is

* Corresponding author at: 28 Fuxing Road, Department of Pathophysiology, PLA General Hospital, 100853 Beijing, China.
E-mail address: xiuhualiu98@163.com (X. Liu).

https://doi.org/10.1016/j.lfs.2019.116591
Received 15 February 2019; Received in revised form 6 June 2019; Accepted 18 June 2019
Available online 20 June 2019
0024-3205/

regulated and influenced by a variety of internal and external factors [11,12]. When depolymerization is dominant, the functional F-actin patterns are always characterized as short, broken actin filaments, which may lead to endothelial injury, including apoptosis, necrosis, and decreased viability, as well as endothelial dysfunction.

Calreticulin (CRT) is known as a highly conserved endoplasmic reticulum (ER)-luminal Ca^{2+}-binding protein, with multiple sublocations [13] and functions [14] in eukaryotic cells. We previously reported that S-band microwave radiation induced human microvascular endothelial cell (HMEC) injury, accompanied by actin cytoskeleton destruction, could be alleviated by application of CRT [7,15]. Other researchers also reported the protective role of CRT on endothelial cells, maintaining the stability of the actin cytoskeleton [16], suggesting a potential role of CRT in radiation protection. However, the underlying mechanisms are unknown.

Protein acetylation is a posttranslational modification catalysed by a wide range of acetyltransferases in the nucleus and cytoplasm [17]. Maturation and maintenance of actin's structure and function often requires N-terminal acetylation [10], and protein acetylation is critical for the regulation of actin polymerization and its stability [14,18]. Recently, CRT was found to be an acyltransferase [19] with many substrates, including glutathione S-transferase, acetyl coenzyme A [19], NADPH, cytochrome *c* reductase, and nitric oxide synthase [19,20].

Therefore, we studied the effects of CRT on HMEC injury, and investigated whether CRT-acetylated actin monomers polymerized to F-actin filaments and which residues of CRT were involved in its acetyltransferase role in HMECs exposed to microwave radiation.

2. Materials and methods

2.1. Preparation of human recombinant active CRT and its P-domain mutant

Based on the human CRT mRNA sequence (NM_004343), the last 4 amino acids (KDEL), which comprise the endoplasmic reticulum retention signal in the C-terminal, and the first 17 amino acids of the leader peptide were both removed to ensure expression and activity in the cytoplasm. We then added a restriction endonuclease site, *Eco*RI, Kozak sequence, and an artificial signal peptide before the 18th amino acid in the N-terminal. We also add a six-histidine (his-) tag, stop codon, and another restriction endonuclease site, *Hind*III, after the 418th amino acid in the C-terminal. Accordingly, we performed codon optimization and synthesized the DNA sequence, then cloned it into the pUC57 vector; this was single-enzyme digested by *Eco*RV to construct a eukaryotic expression vector. Similarly, we cloned the plasmid vector containing the P-domain mutant CRT protein, in which the Lys-206 and -207 were mutated to arginine.

Transfection grade plasmids of CRT and P-domain mutant CRT were prepared for transient expression in Chinese hamster oocytes (CHO)-ExpiCHO cells (Life Technologies, Carlsbad, CA, USA) [21]. Cells were grown in serum-free FreeStyle™ CHO Expression Medium (Life Technologies, Carlsbad, CA, USA). The cells were maintained in Erlenmeyer Flasks (Corning Inc., Acton, MA, USA) at 36.8 °C with 8% CO_2 on an orbital shaker (VWR Scientific, Chester, PA, USA). One day before transfection, the cells were seeded at a density of 3×10^6 cells/mL in Erlenmeyer Flasks. On the day of transfection, the recombinant plasmids were transiently transfected into 1 L suspension CHO-S cell cultures. The cell culture supernatant collected on day 6–8 was used for purification. Cell culture broth was centrifuged and loaded onto HisTrap™ FF Crude 5 mL (Cat. No. 17-5286-01, GE Healthcare, Sweden) at 3.0 mL/min. After washing and elution, the eluted fractions were pooled and buffer exchanged to phosphate buffered saline, pH 7.4. The purified protein was analyzed by high performance liquid chromatography, SDS-PAGE and western blot, and the concentration, purity, and endotoxin content were measured.

2.2. Cell culture, microwave irradiation, and grouping

HMECs were cultured and exposed to S-band high-power microwaves of 2.856 GHz which at a mean power density of 60 mW/cm^2 for 6 min as we previously reported [7,13]. To assess the impact of microwave radiation on the HMECs, we divided cells into four groups, 1) natural control group (NC): HMEC cells were cultured normally in a 5% CO_2 incubator at 37 °C for a further 24 h; 2) the microwave radiation group (MR): HMECs were exposed to microwave radiation of 60 mW/cm^2 for 6 min, then moved to the 5% CO_2 incubator at 37 °C for a further 24 h; 3) CRT incubation group (CRT): HMECs were incubated with the recombinant active CRT at a concentration of 25 pg/mL for 24 h; 4) group pre-incubated with CRT before microwave irradiation (CRT + MR): HMECs were pre-incubated with CRT (25 pg/mL) for 30 min before irradiation and then treated as group 2).

2.3. Cell survival rate

We seeded the cells at a density of 3×10^4 cells/cm^2 in 24-well plates. At the end of the experiment, we digested the HMECs with 0.02% trypsin and resuspended the cells with 0.1 mol/L phosphate buffered saline. We mixed the cells with an equal volume of 4% trypan blue dye and observed them under a light microscope (Olympus, CK-2, Japan). We counted the live cells with intact cell membranes, which were not coloured by trypan blue, then calculated the survival rate. The experiments were repeated three times. In each time, 500–600 cells were counted in one group.

2.4. Cell viability

Using a cell counting kit-8 (CCK-8; Beyotime, Nantong, China), cells were seeded in 96-well plates at a density of 5×10^3/100 μL/well. Eight parallel wells were placed in one group. At the end of the experiment, cells were incubated with CCK-8 for 4 h. Samples were measured at 450 nm wavelength using a microplate reader (Tecan Infinite f200 Pro; Tecan Group Ltd, Männedorf, Switzerland).

2.5. Cell apoptosis

HMECs were seeded at a density of 1×10^4 cells/cm^2 on 1% gelatin-coated coverslips within 24-well plates. At the end of experiment, apoptosis was detected as we previously reported [22]. Briefly, we used a DeadEnd™ Fluorometric TUNEL System (Promega, Madison, WI, USA) following the manufacturer's protocol. The coverslips were mounted on glass slides with mounting medium and DAPI. At least ten randomly chosen fields with 100 cells were scored, and the number of TUNEL-positive cells was expressed as a fraction of the total cell number.

2.6. Permeability study

According to the literature [23,24], we seeded the endothelial cells on the 1% gelatin-coated transwell filter (Corning-Costar, USA) at a concentration of 5×10^4 cells/cm^2, when reaching confluence, cells were changed in fresh Phenol red-free DMEM and treated with CRT as well as microwave radiation. Paired experiments were adopted in each group. When 24 h after radiation, 100 μL FITC-albumin (Sigma-Aldrich) at a concentration of 1 mg/mL were added gently to the abluminal chamber and incubated for 45 min in a humidified atmosphere with 5% CO_2 at 37 °C. 100 μL sample was removed from each abluminal (bottom) and luminal (top) chamber and the fluorescence intensity was measured at Ex/Em = 490/520 nm wavelength with a fluorescence microplate reader (Varioskan LUX, Thermo, USA). We also measured the volume of medium in the abluminal chamber. These concentrations were then used in the following equation to determine the permeability coefficient of albumin (Pa), $Pa = [A] / t \times 1 / A \times v / [L]$, where [A] = abluminal concentration which could be calculated as

fluorescent intensity, t = time in s, A = area of membrane in cm^2, V = volume of abluminal chamber, and [L] = luminal concentration that showed as fluorescent intensity.

2.7. Fluorescence assay

To label VE-cadherin, HMECs were seeded on coverslips, contained within 24-well plates, at a density of $2 \times 10^4/cm^2$, and subjected to immunocytofluorescence assay as described previously [25]. Briefly, the paraformaldehyde-fixed cells were incubated with mouse anti-VE-cadherin monoclonal antibody (1:100; Abcam, USA) at 4 °C overnight, and then incubated with donkey anti-mouse Alexa Fluor 488 (Thermo, USA) at room temperature for 2 h in the dark.

To label F-actin, HMECs were seeded at a density of 1×10^4 cells/cm^2. Cells were stained with fluorescein isothiocyanate (FITC)-labelled phalloidin (final concentration 0.33 μmol/L; Sigma-Aldrich, USA) as previously described [25]. These coverslips were then counterstained with DAPI, mounted on glass slides, and observed under a laser scanning confocal microscope (Zeiss, 510-Meta, Germany).

2.8. Western blot

As we reported previously [25], Samples containing 50 μg of protein were separated on 10% acrylamide gels, transferred to nitrocellulose membranes, and blocked with 5% non-fat milk in Tris-buffered saline Tween (20 mmol/L Tris-HCl, pH 7.5, 137 mmol/L NaCl, and 0.1% Tween 20). Membranes were incubated with antibodies against rabbit anti-pan-actin (1:500, Cell Signaling Technology, USA), rabbit anti-acetylated lysine (1:500, Cell Signaling Technology), rabbit anti-VE-cadherin (1:200, Santa Cruz, Dallas, Tex, USA), and rabbit anti GAPDH (1:500; Santa Cruz). Membranes were further incubated with horseradish peroxidase-conjugated secondary antibodies for 1 h at room temperature, and visualized using an enhanced chemiluminescence kit (Santa Cruz).

2.9. F-actin polymerization

The Actin Polymerization Biochem Kit (Cytoskeleton Inc., USA) is based on the enhanced fluorescence of pyrene-conjugated actin that occurs during polymerization, according to the operating manual as well as literature reports [26].

The kinetics of fluorescence enhancement from 0 to 60 min was evaluated by measuring fluorescence of the samples using a fluorimeter (Enspire-2300, PerkinElmer, USA), and the parameters are given in Table 1. The initial rate of polymerization in the linear phase of each reaction was estimated by linear regression method.

2.10. Coimmunoprecipitation

Protein interaction was evaluated using a protein G-immunoprecipitation kit (Roche, Switzerland). Following the instruction manual, precleared bait proteins, the purified CRT, and purified actin (> 99% pure from human platelet; Cytoskeleton Inc.) were subjected to goat anti-CRT antibody and mouse anti-pan-actin antibody precipitation overnight at 4 °C, respectively. Immune complexes captured by protein G–Sepharose beads were incubated with the prey proteins actin and CRT. Meanwhile, equal amounts of the goat and mouse IgG solutions were employed in place of the immunoprecipitation antibodies as negative controls. Whole-cell lysates derived from normal cultured HMECs were used as input. Ultimately, the immunoprecipitated samples were subjected to the western blot assay.

Table 1
Parameter settings of the fluorimeter used to measure the enhanced fluorescence of pyrene-conjugated actin.

Measurement type	Kinetic	120 cycles, 60 s interval time
Fluorescence wavelengths	Ex.	350 nm
	Em.	410 nm
Gain	100	
Reads per well	1	
Fluorescence reading from	Top	
Integration	0–40 μs	
Shaking	5 s	Medium, orbital, once before first read
Plate type	Greiner	Greiner GRE96fb (flat, black)

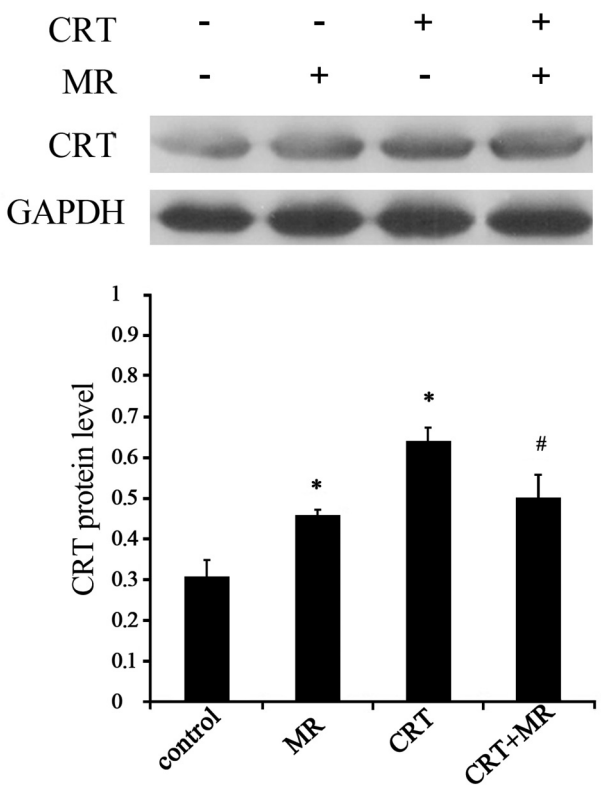

Fig. 1. Relative expression of endothelial calreticulin (CRT) normalized to GAPDH, n = 3; $^*P < 0.05$ vs. NC; $^{\#}P < 0.05$ vs. MR.

2.11. His-tag pull down

Protein interaction was evaluated by the pull-down assay. According to the manual of the Pierce Pull-Down PolyHis Protein:Protein Interaction Kit (Thermo Fisher), the recombinant active human CRT protein was immobilized to the cobalt chelate affinity resin, and then incubated with the putative binding protein actin for 4 h at 4 °C. The beads were then washed three times with Tris-buffered saline (25 mmol/L Tris-HCl, 0.15 mol/L NaCl, pH 7.2), boiled in 1× SDS-PAGE loading buffer (50 mmol/L Tris-HCl, 100 mmol/L dithiothreitol, 0.2% sodium dodecylsulphate, 0.1% bromophenol blue, and 10% glycerol, pH 6.8), and subjected to immunoblotting assay.

2.12. In vitro transacylation reaction and mutant experiment

As reported [16], 10 μg CRT acetyltransferase or its P-domain mutant protein ($^{\triangle}$CRT) were incubated with the acetyl group donor acetyl CoA (final concentration 100 μmol/L) and 30 μg putative actin substrate, in a buffer containing 500 mmol/L KCl, 20 mmol/L $MgCl_2$, 0.05 mol/L guanidine carbonate, and 10 mmol/L ATP, and incubated for 30 min at 37 °C in a shaking water bath. SDS-PAGE loading buffer 1× was added to stop the reaction, and the mixture was used to detect the acylation of actin by western blot.

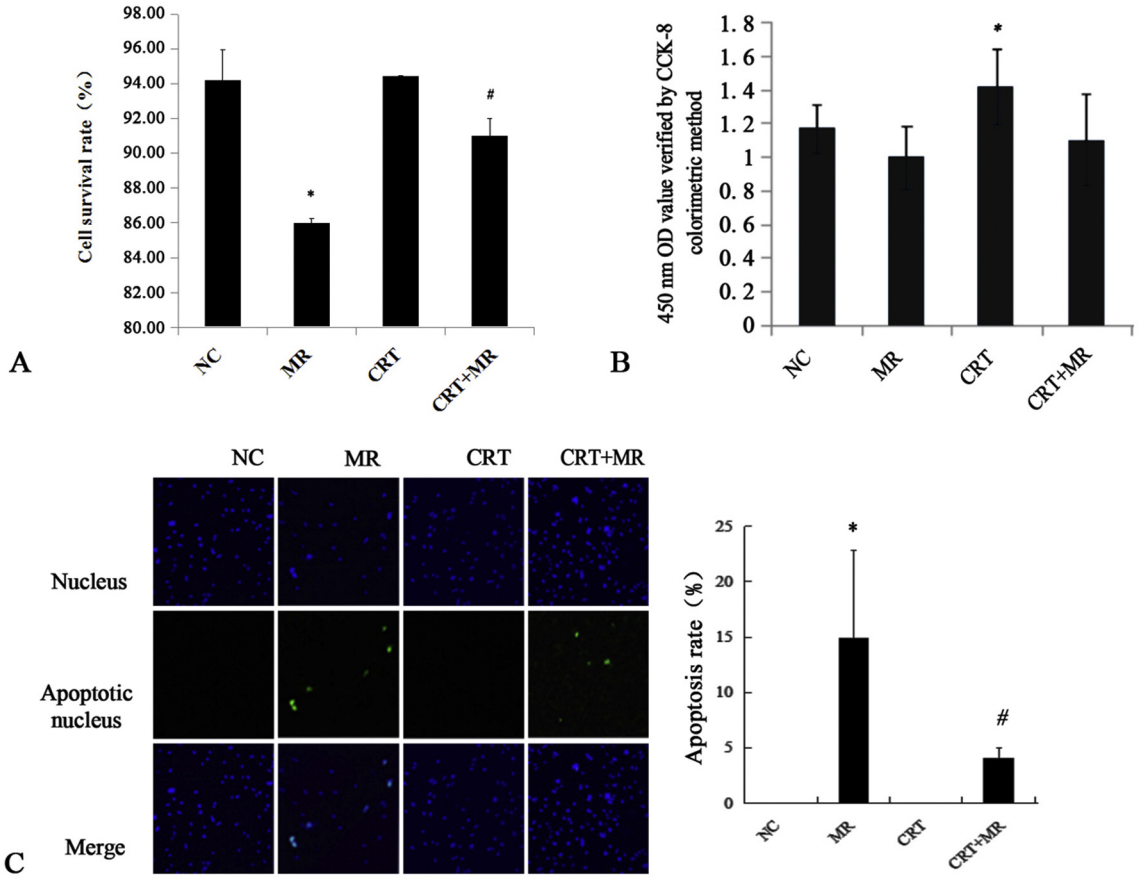

Fig. 2. Effects of microwave radiation and CRT incubation on the HMECs injury.
The protective role of CRT was evaluated by cell survival rate assessed by Trypan blue exclusion assay (A), cell viability measured by cell counting kit-8 reagent (B), and apoptosis rate evaluated by TUNEL assay (C). n = 3, $^{*}P < 0.05$ vs. NC; $^{\#}P < 0.05$ vs. MR.

2.13. Statistical analysis

Data tested to be normally distributed are expressed as the mean ± SD. One-way analysis of variance was performed, followed by Bonferroni method post-hoc analysis (SPSS 17.0) to compare the means of two different treatment groups. The level of significance was set to $P < 0.05$. The semi-quantitative data of actin expression level and F-actin fluorescence intensity were analyzed by Pearson's product-moment correlation coefficient analysis.

3. Results

3.1. Microwave radiation increases endogenous CRT expression

The endogenous CRT, an endoplasmic reticulum stress (ERS)-related molecule, was significantly up-regulated after the microwave radiation, as shown in Fig. 1.

3.2. Extracellular CRT alleviates microwave radiation-induced endothelial cell injury

As shown in Fig. 2A, using the trypan blue exclusion method we found that the survival rate of normal cultured HMECs was 94.20 ± 1.75%, significantly higher than that of the microwave-irradiated cells, whose survival rate was 85.98 ± 0.25% ($P < 0.05$). CRT incubation did not affect the survival rate of HMECs; however, the survival rate of cells preincubated with CRT before radiation was 91.01 ± 0.99%, significantly higher than that of the radiation group ($P < 0.05$). As shown in Fig. 2B, using a cell counting kit-8 the cell viability of the radiation group was significantly lower than that of the normal control group ($P < 0.05$), while incubation with CRT increased cell viability ($P < 0.05$ vs. NC); specifically, pre-incubation with CRT significantly increased cell viability compared with the radiation group ($P < 0.05$). We then measured the apoptosis rate; as shown in Fig. 2C, in the normal control group, the apoptosis rate was 0.00, while that of the radiation group was 14.88 ± 8.00% ($P = 0.000$). Incubation with CRT did not affect the apoptosis rate; however, CRT pre-incubation significantly reduced the apoptosis rate to 2.60 ± 0.68%.

3.3. Extracellular CRT inhibits microwave radiation-induced increase in permeability

We examined whether CRT had a protective effect on endothelial monolayer permeability. As shown in Fig. 3A, in microwave-challenged cells, the permeability was significantly increased compared with the control group ($P < 0.05$). However, when CRT was added to the cells at concentrations of 25 pg/mL prior to exposure to microwave, the endothelial cell-permeability was lower than those of the microwave radiation group ($P < 0.05$).

To evaluate endothelial barrier function, we detected the expression and morphology of VE-cadherin, which indicates the integrity of endothelial adhesion junctions. VE-cadherin expression was significantly downregulated in microwave-irradiated HMECs ($P < 0.05$ vs. NC), but significantly upregulated in the CRT-pre-incubated microwave-irradiated group, compared with the radiation group (Fig. 3B).

With immunocytofluorescence staining, the normal control group showed distinct continuous signals distributed at the surface membrane cells, while the microwave-irradiated group showed obvious

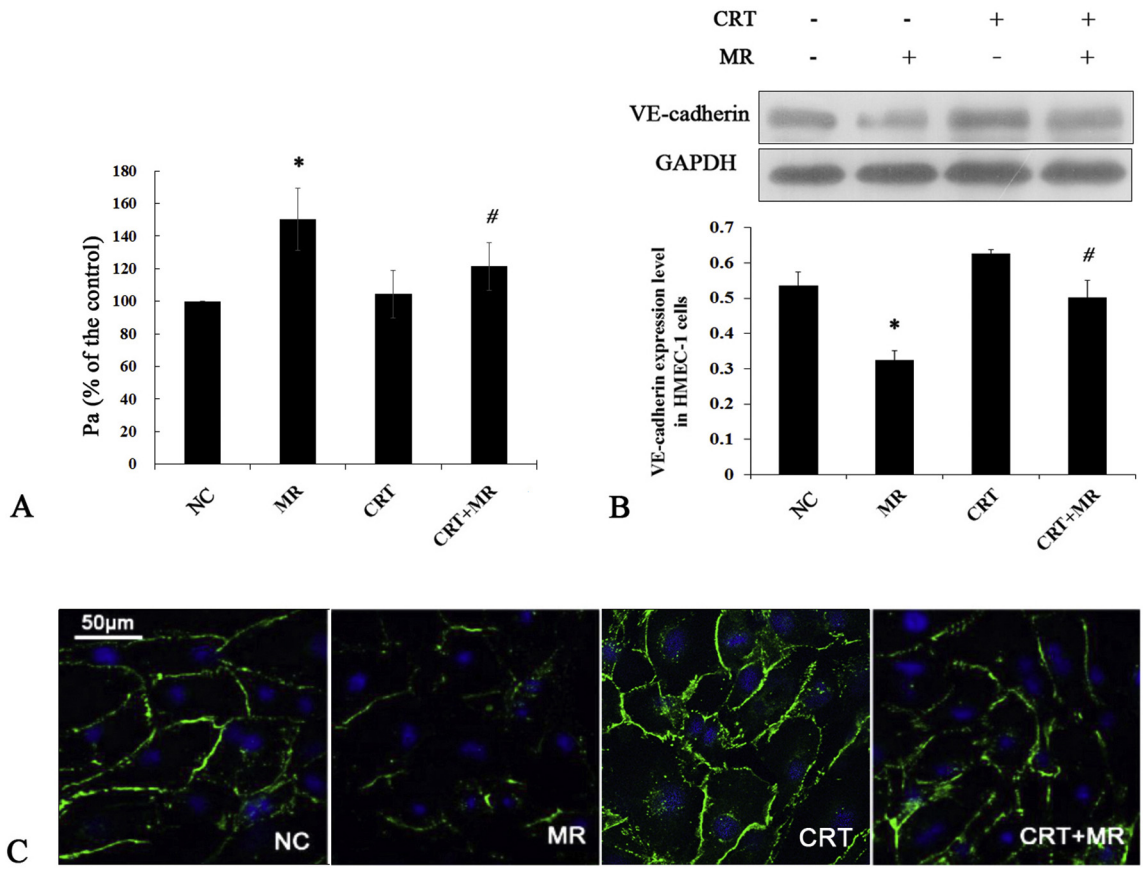

Fig. 3. Effects of microwave radiation and CRT incubation on the HMECs hyperpermeability.
Permeability (Pa) of HMECs culture (expressed as percentage of control cells). n = 3; $^{*}P < 0.05$ vs. NC; $^{\#}P < 0.05$ vs. MR (A). Relative expression of endothelial intercellular molecule vascular endothelial (VE)-cadherin (normalized to GAPDH), n = 3; $^{*}P < 0.05$ vs. NC; $^{\#}P < 0.05$ vs. MR (B). Cellular distribution of VE-cadherin detected by immunocytofluorescence with the VE-cadherin antibody, n = 3; scale bar = 50 μm (C).

destruction of continuous fluorescent signals; pre-incubation with CRT noticeably improved the radiation-weakened fluorescence (Fig. 3C).

3.4. Extracellular CRT inhibits microwave radiation-induced actin depolymerization

Using phalloidin-FITC staining to detect the actin cytoskeleton, normal cultured HMECs contained F-actin filaments mainly arranged as cortical networks and stress-fibres in the cytosol. However, actin assembly in the irradiated cells displayed a short or punctate pattern. Compared with the normal control, CRT-incubated cells showed thicker and longer patterns, which were orderly arranged in the cytosol. Pre-incubation with CRT significantly alleviated the radiation-destroyed F-actin assembly (Fig. 4A).

To investigate the impact of CRT on F-actin polymerization, we recorded the kinetics of fluorescence enhancement from 0 to 60 min. The enhanced fluorescence intensity between 10 and 15 min was thought to increase in a linear manner (Fig. 4B). The initial rate of polymerization in the linear phase from 10 to 15 min of each reaction was estimated by linear regression. As shown in Fig. 4C, the enhanced fluorescence of pyrene-conjugated actin that occurs during polymerization significantly decreased after microwave irradiation (MR = 496.45 ± 23.41 vs. NC = 504.86 ± 10.92; $P < 0.05$). CRT-incubation significantly enhanced the fluorescence (536.13 ± 8.29), and pre-incubation with CRT significantly restored the radiation-reduced fluorescence (518.77 ± 6.58; $P < 0.05$ vs. MR).

3.5. Extracellular CRT rescues downregulation of actin acetylation induced by high-power microwave radiation

As shown in Fig. 5, using western blot analysis with pan-actin and acetylated lysine antibodies, we detected both bands at the same level (45 kDa). Compared with the normal control, the expression of acetylated actin significantly decreased after microwave-irradiation ($P < 0.05$). CRT-incubation noticeably increased the actin acetylation level, and reversed the radiation-downregulated acetylated actin level ($P < 0.05$ vs. MR). Remarkably, the acetylation level of actin was positively correlated with the degree of actin polymerization (r = 0.996; $P < 0.05$).

3.6. Recombined eukaryotic CRT interacts with actin in vitro

In coimmunoprecipitation experiments, we found that the eukaryotic-derived purified CRT was baited by the goat anti-CRT polyclonal antibody, but the goat IgG largely was not (Fig. 6A). Similarly, the eukaryotic-derived actin protein was baited by the mouse anti-pan-actin monoclonal antibody, but the mouse IgG largely was not (Fig. 6B). Actin protein was readily coprecipitated by goat anti CRT polyclonal antibody but not by mouse IgG (Fig. 6A), and purified CRT was readily coprecipitated by mouse anti-pan-actin monoclonal antibody but not by goat IgG (Fig. 6B).

The his-tag pull-down assay revealed that the purified CRT was successfully immobilized on the cobalt chelate beads; however, no interacting protein was observed when only beads were used as a control (Fig. 7A). Pull-down assay also showed a much higher level of actin proteins detected by actin antibody in the CRT-treated group, than in

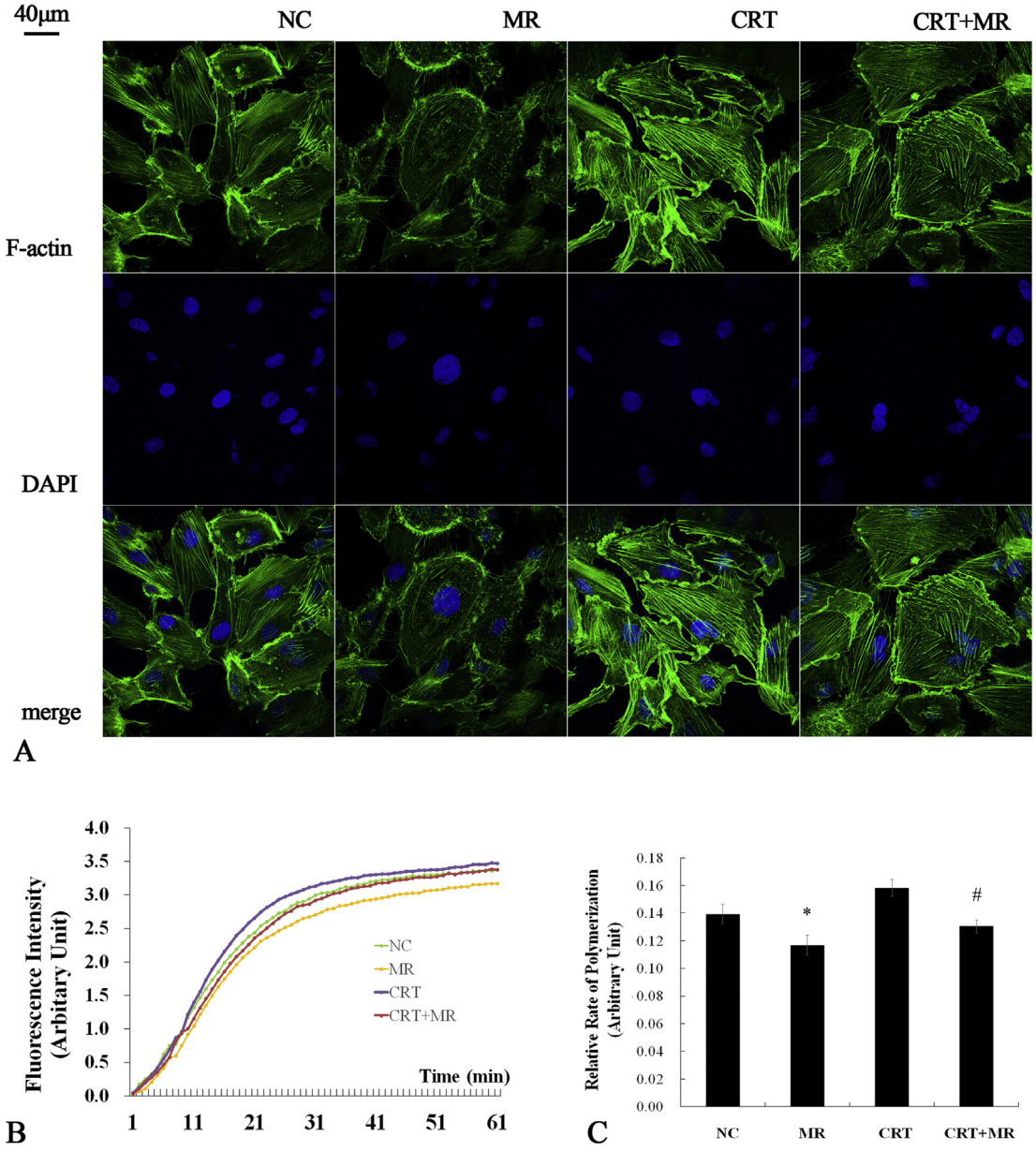

Fig. 4. Effects of microwave radiation and CRT incubation on F-actin arrangement and polymerization in HMECs.
F-actin (green) and nuclei (blue) double-staining with the fluorescein isothiocyanate-phalloidin and DAPI, respectively. n = 3; scale bar = 40 μm (A). Enhanced fluorescence of pyrene-conjugated actin representing polymerization measured for 60 min (B). The slop of fluorescence intensity between 10 and 15 min (during which period the enhanced fluorescence was thought to increase in a linear manner). n = 3; $^{*}P < 0.05$ vs. NC; $^{\#}P < 0.05$ vs. MR (C). (For interpretation of the references to colour in this figure legend, the reader is referred to the web version of this article.)

groups without CRT application (Fig. 7B).

3.7. CRT transacetylase catalyses acetylation of actin

To further elucidate the effect of CRT acyltransferase on actin, we performed an ex vitro acetylation assay. With acetyl coenzyme A (AcCoA) added as the acetyl group donor in the CRT transacylation reaction system, acylated actin bands at 45 kDa were detected using an anti-acetyl lysine antibody. The actin band was observed when CRT was used without AcCoA, but the band density was much lower ($P < 0.05$). We did not detect any positive band in the absence of actin, although in the CRT and acyl groups donors were still sufficient. To identify the acyltransferase specificity of the proline-rich domain (P-domain) in CRT protein, we utilized a P-domain mutant CRT ($^{\triangle}$CRT) instead of the recombinant CRT. We detected almost no band in the mutant $^{\triangle}$CRT group, although actin and AcCoA were provided (Fig. 8).

4. Discussion

Exposure of human beings to electromagnetic radiations has been listed as an environmental hazard by the United Nations Conference on the Human Environment [27]. The S-band microwave (2–4 GHz) is more widely applied in daily life and has raised concerns about its hazard to health [1]. The cardiovascular system, one of the most susceptible biological systems to microwave radiation, might be impaired by certain intensities of S-band microwaves, leading to malformed capillaries and decreased blood flow. The large number of endothelial cells contributes greatly to the selective endothelial barrier between blood and tissue. Injury and dysfunction induced by microwave radiation may increase vascular permeability, leading to plasma protein

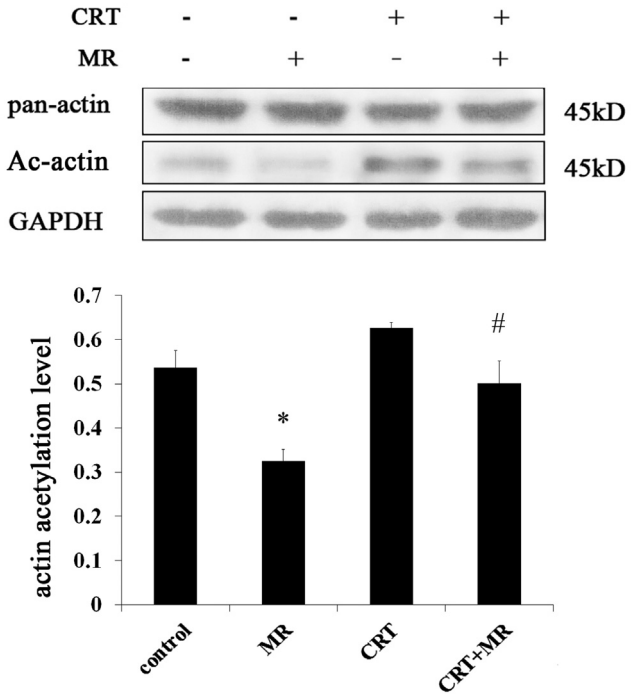

Fig. 5. Effects of microwave radiation and CRT incubation on total actin and acetylated actin expression.
Relative expression levels of pan-actin and acetylated actin bands and their semi-quantitatively calculation. n = 3, $^{*}P < 0.05$ vs. NC group; $^{\#}P < 0.05$ vs. MR group.

leakage and material-energy exchange dysfunction, subsequently resulting in oedema, inflammation, and many other kinds of homeostasis imbalance. It is suggested that protection of endothelial cells could be a critical approach for microwave radiation damage prevention.

We subjected HMECs to 60 mW/cm^2 intensity of S-band microwave radiation for 6 min, which decreased cell survival and viability and increased apoptosis, indicating that this intensity and duration of microwave exposure are sufficient to induce cell injury. We further found that radiation disrupted the actin cytoskeleton and the continuous distribution of VE-cadherin, the intercellular junction molecule specifically expressed in endothelial cells that plays a critical role in adhesion junction formation to stabilize endothelial cell contact [28]. The adhesion junctions depend on their connection to the actin cytoskeleton, and dynamic alterations of the actin cytoskeleton have a profound impact on the regulation of endothelial barrier functions and modulate vascular permeability [29,30]. Therefore, we evaluated the actin cytoskeleton and demonstrated that high-power microwave radiation inhibited actin polymerization, thus disrupting the F-actin arrangement. It is suggested that polymerization of F-actin is of great importance to improve the stability of actin filaments and to subsequently maintain the endothelial barrier against radiation injury.

CRT is found involved in the adaptive response of brain capillary endothelial cells to hypoxia and reoxygenation [31]. We also previously reported that exogenous pretreatment of CRT protein could alleviate microwave radiation-induced endothelial injury [13]. In this study, HMECs was incubated with CRT prior to high-power microwave irradiation; CRT effectively increased cell survival and viability, reduced apoptosis, enhanced VE-cadherin expression and continuity, and ameliorated F-actin malalignment and filament rupture. This indicates that the extracellular CRT may alleviate radiation injury by stabilizing the F-actin filaments.

CRT is a highly conserved and multifunctional protein, mainly resident in the endoplasmic reticulum (ER), known for its lectin-like chaperoning and Ca^{2+} storage. In recent years, it has been reported that CRT also exists in the surface of cell membrane, cytoplasm, nucleus, and extracellular matrix, known as “non-endoplasmic reticulum calreticulin (non-ER CRT)”, with the functions of signaling, regulation of gene expression, cell adhesion, tumour cell recognition, and, particularly, wound healing [11,32]. There are two major opinions on the sources of cytosolic non-ER CRT, one is that the cytosolic CRT may derive from nuclear CRT excluded from nucleus by binding to some proteins with the nuclear export signals (NES) [33]. On the other hand, the cytosolic CRT may be a truncation of ER-resident CRT which escape from the ER by being cut off its classical ER retention signal at the C-terminal KDEL sequence [34]. By using western blot, we found that the endogenous CRT significantly increased after microwave radiation but without the same protective role as the extracellular CRT. The increased CRT expression may be due to the microwave radiation-induced endoplasmic reticulum stress (ERS). This kind of CRT is mainly resident in the ER but not distributed in the cytosol where it is named as “non-ER CRT” with the acetyl transferase activity. The different localizations of CRT might explain the reason why CRT is up-regulated but still fail to rescue the radiation injury. We previously found that extracellular applied CRT enhanced the cytosolic non-ER CRT expression [7], indicating that extracellular CRT may promote the release of non-ER CRT.

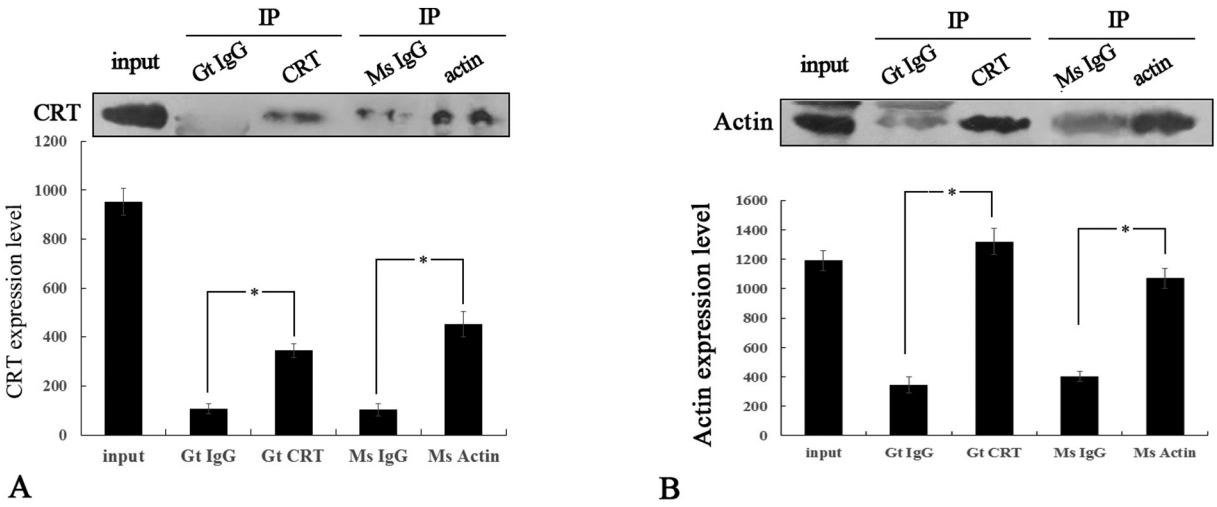

Fig. 6. Interaction between CRT and actin verified by coimmunoprecipitation assay.
By using whole cell lysates as prey, either CRT or actin purified protein was used as bait, and the immunoprecipitation complex was specifically identified by CRT (A) and actin (B) antibodies. Goat and mouse IgG antibodies were used as negative controls. n = 3, $^{*}P < 0.05$.

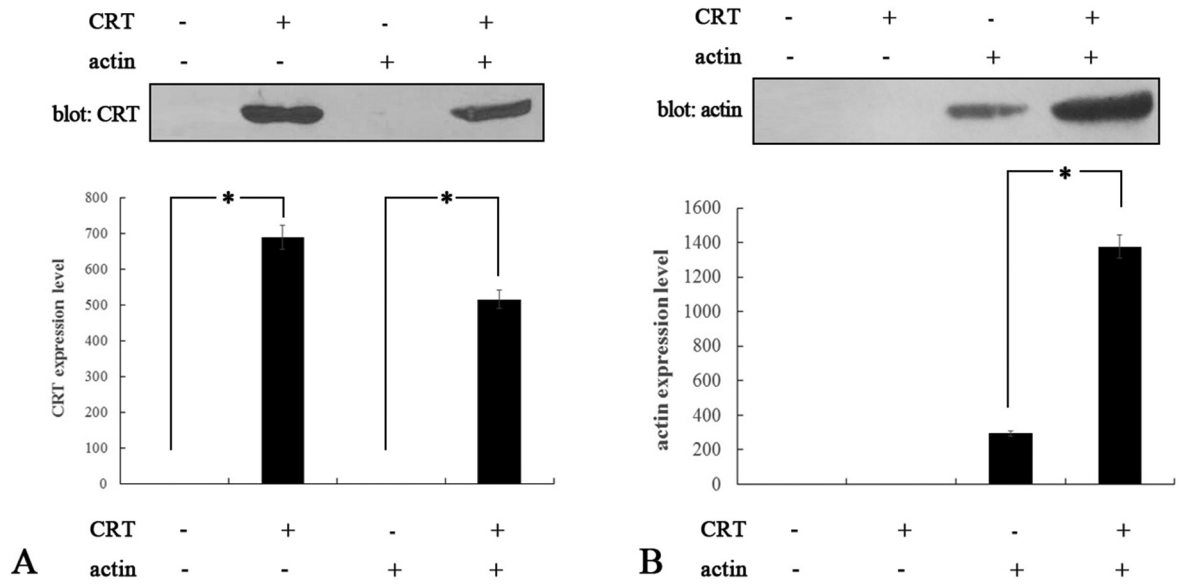

Fig. 7. Interaction between calreticulin (CRT) and actin verified by pull-down assay.
The polyhistidine-tagged bait protein CRT was immobilized to a cobalt chelate affinity resin to identify its putative binding partner, actin. The beads-bait-prey complexes were detected by CRT antibody (A) and pan-actin antibody (B), respectively. n = 3, $^*P < 0.05$.

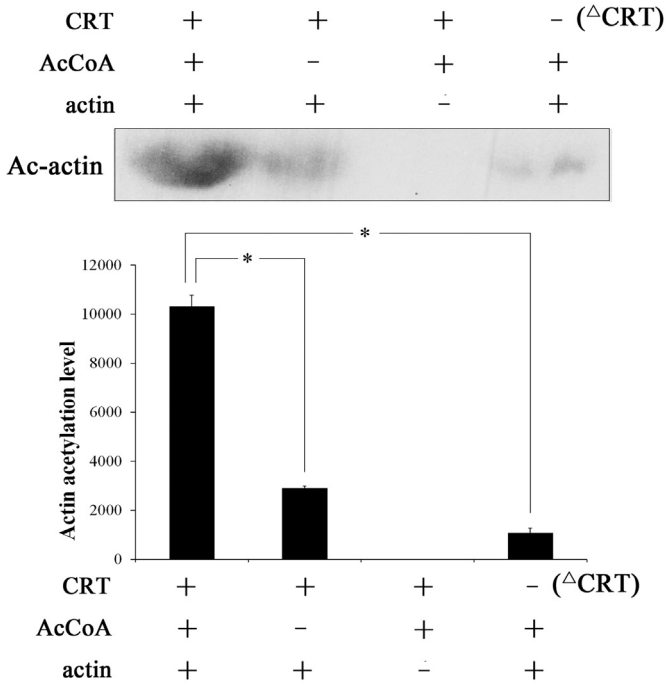

Fig. 8. Demonstration of active CRT acyltransferase specificity in its P-domain.
Active CRT, or its P-Domain mutant CRT protein was mixed with actin and AcCoA or not. The acylation reaction mixtures were separated by SDS-PAGE and blotted for the detection of acetylated actin. n = 3, $^*P < 0.05$.

Theoretically, CRT is a critical extracellular signal in many pathways. For example, thrombospondin bounds to CRT-LRP1 complex and promoted FAK phosphorylation [35]. We also found that the increased CRT on the membrane of cell surface upregulated integrin-α and activated its downstream, the FAK/Akt mediated pathway [15]. It suggests that extracellular CRT might conduct signals promoting CRT expression from extracellular to intracellular and facilitate the non-ER CRT release (wherever from nucleus or ER) through such signal transduction pathways.

Recently, the novel role as an acyltransferase of cytosolic non-ER CRT has become an attractive target for investigations [16,19]. Acetylation is a common, reversible, and well-controlled post-translational modification, which occurs mainly in the lysine residues of ε-NH_2 [17]. Acetylation is of great significance in eukaryotic cells, which require precise regulation of metabolism to maintain homeostasis. Actin is one such protein regulated through post-translational modifications [10]. It has been reported that maintenance of actin's structural and functional properties often requires N-terminal acetylation. The N-terminus of actin protein contains at least two sites that can be acetylated, lys-326 and -328 [36]. Acetylated monomer actins more efficiently participate in the assembly of F-actin [37]. The acetylation modification could reduce the positive charges at the N-terminal of actin, forming a negatively charged cluster that plays a pivotal role in the maintenance of actin cytoskeleton stability [38]. Through correlation analysis, we found that the actin acetylation level was positively correlated with the degree of actin polymerization. Stated thus, actin might serve as a novel substrate of CRT acyltransferase, and may be acetylated to maintain its stability and polymerization.

To demonstrate that actin is acetylated by CRT, most importantly, we had to ensure that CRT interacts with actin directly. The data from coimmunoprecipitation and pull-down assays confirmed the direct interaction between CRT and actin. In the pull-down assay, we detected a very weak actin band in the actin control group without added CRT. We speculated that the purified active actin derived from human platelets had a similar spatial poly-histidine structure to the six-histidine-tagged bait protein, and might have a weak nonspecific binding with the cobalt chelate resin.

The ex vitro acetyltransferase reaction to investigate whether actin could be an enzymatic substrate of CRT revealed that CRT transferred acetyl groups from its known substrate, AcCoA, to the actin protein. Interestingly, a certain degree of expression of acetyl-actin was still detected without acetyl group donor provision, but the detected band was considerably weaker, probably owing to the autoacetylated CRT acting as a stable intermediate in the protein acetyltransferase reaction [39].

Many acetyl sites have been identified in CRT, including the lysine residues Lys-48, -62, -64, -153, and -159 in the N-domain and -206, -207, -209, and -238 in the P-domain following the N-domain. None of the lysine residues in the C-domain were observed to be covalently modified by acetylation [40–42]. However, the P-domain alone was

exclusively characterized as possessing acetyltransferase activity, mainly because of its best ranked docking position with lowest binding energy. Specifically, Lys-206 and -207 showed more evidence of the CRT acetylation reaction [17]. For this reason, we employed a P-domain mutant △CRT (both lys-206 and -207 were mutated to arginine) protein instead of CRT to evaluate the acetylation activity of the P-domain on actin. The result showed a very weak positive band when △CRT protein was used, indicating that lys-206 and -207 contribute greatly to this transacylation reaction. However, we cannot exclude the possibility that other acetylation sites exist which contribute to CRT acetyltransferase activity.

5. Conclusions

In conclusion, we demonstrated actin to be a novel substrate of CRT acyltransferase. CRT directly transfers acetyl groups to actin, mainly through lys-206 and -207 residues in the P-domain. The CRT-acetylated actin is promoted and polymerized to F-actin, strengthening the cytosolic and cortical actin filaments, which connect with the crucial intercellular molecule VE-cadherin in the lateral cell membrane. Thus, HMEC injury was attenuated during the high-power microwave exposure. These findings further enrich the mechanism repertoire of CRT-induced cytoprotection, and suggest a novel therapeutic target for microwave radiation-related diseases with endothelial dysfunction. Further studies are needed to elucidate the exact effect and potential biological mechanisms of CRT in the actin acetylation of HMECs during microwave radiation.

Acknowledgements

Funding

This work was supported by the National Natural Science Foundation of China (No. 31771287) and National Basic Research Program of China (973 Program) (No. 2015CB554402).

Declaration of competing interest

Xiaoreng Wang, PhD: None.
Tianqi Tao, MS: None.
Dandan Song, BS: None.
Huimin Mao, PhD: None.
Mi Liu, PhD: None.
Jianli Wang, MS: None.
Xiuhua, PhD: None.

Author contribution

Conceptualization: Xiaoreng Wang, PhD and Xiuhua, PhD
Data analysis: Tianqi Tao, MS; Dandan Song, BS; Huimin Mao, PhD; Mi Liu, PhD
Funding acquisition: Xiuhua Liu, PhD
Methodology: Xiaoreng Wang, PhD; Tianqi Tao, MS; Dandan Song, BS; Huimin Mao, PhD; Mi Liu, PhD; Jianli Wang, MS
Supervision: Xiaoreng Wang, PhD; Xiuhua Liu, PhD
Validation: Xiaoreng Wang, PhD; Xiuhualiu, PhD
Writing - original draft: Xiaoreng Wang, PhD
Writing - review & editing: Xiuhua Liu, PhD.

References

[1] H. Wang, S. Tan, J. Dong, J. Zhang, B. Yao, X. Xu, Y. Hao, C. Yu, H. Zhou, L. Zhao, R. Peng, iTRAQ quantitatively proteomic analysis of the hippocampus in a rat model of accumulative microwave-induced cognitive impairment, Environ. Sci. Pollut. Res. Int. 26 (2019) 17248–17260 Pubmed: 31012066.

[2] B. Bilgici, S. Gun, B. Avci, A. Akar, K. Engiz, B, What is adverse effect of wireless local area network, using 2.45 GHz, on the reproductive system, Int. J. Radiat. Biol. 94 (2018) 1054–1061 (PubMed: 30028652).

[3] R. Meena, K. Kumari, J. Kumar, P. Rajamani, H.N. Verma, K.K. Kesari, Therapeutic approaches of melatonin in microwave radiations-induced oxidative stress-mediated toxicity on male fertility pattern of Wistar rats, Electromagn. Biol. Med. 33 (2014) 81–91 (Pubmed: 22134878).

[4] P. Chauhan, H.N. Verma, R. Sisodia, K.K. Kesari, Microwave radiation (2.45 GHz)-induced oxidative stress: whole-body exposure effect on histopathology of Wistar rats, Electromagn. Biol. Med. 36 (2017) 20–30 (Pubmed: 27362544).

[5] K.K. Kesari, J. Behari, S. Kumar, Mutagenic response of 2.45 GHz radiation exposure on rat brain, Int. J. Radiat. Biol. 86 (2010) 334–343 (Pubmed: 20353343).

[6] S.M. Mortazavi, S.M. Owji, M.B. Shojaei-Fard, M. Ghader-Panah, S.A. Mortazavi, A. Tavakoli-Golpayegani, M. Haghani, S. Taeb, N. Shokrpour, O. Koohi, GSM 900 MHz microwave radiation-induced alterations of insulin level and histopathological changes of liver and pancreas in rat, J. Biomed. Phys. Eng. 6 (2016) 235–242 (Pubmed: 28144593).

[7] W.H. Li, Y.Z. Li, D.D. Song, X.R. Wang, M. Liu, X.D. Wu, X.H. Liu, Calreticulin protects rat microvascular endothelial cells against microwave radiation-induced injury by attenuating endoplasmic reticulum stress, Microcirculation 21 (2014) 506–515 (Pubmed: 24589181).

[8] Y. Li, X. Qu, X. Wang, M. Liu, C. Wang, Z. Lv, W. Li, T. Tao, D. Song, X. Liu, Microwave radiation injuries microvasculature through inducing endoplasmic reticulum stress, Microcirculation 21 (2014) 490–498 Feb 7 [Epub ahead of print] [Pubmed: 24635541].

[9] X.W. Wang, G.R. Ding, C.H. Shi, T. Zhao, J. Zhang, L.H. Zeng, G.Z. Guo, Effect of electromagnetic pulse exposure on permeability of blood-testicle barrier in mice, Biomed. Environ. Sci. 21 (2008) 218–221 (Pubmed: 18714819).

[10] J.R. Terman, A. Kashina, Post-translational modification and regulation of actin, Curr. Opin. Cell Biol. 25 (2013) 30–38 (Pubmed: 23195437).

[11] G. Kustermans, J. Piette, S. Legrand-Poels, Actin-targeting natural compounds as tools to study the role of actin cytoskeleton in signal transduction, Biochem. Pharmacol. 76 (2008) 1310–1322 (Pubmed: 18602087).

[12] Iskratsch T, Lange S, Dwyer J, Kho AL, dos Remedios C, Ehler E, Formin follows function: a muscle-specific isoform of FHOD3 is regulated by CK2 phosphorylation and promotes myofibril maintenance, J. Cell Biol. 191 (2010) 1159–1172. (Pubmed: 21149568).

[13] S. Johnson, M. Michalak, M. Opas, P. Eggleton, The ins and outs of calreticulin: from the ER lumen to the extracellular space, Trends Cell Biol. 11 (2001) 122–129 (Pubmed: 11306273).

[14] P. Singh, P. Ponnan, N. Priya, T.K. Tyagi, M. Gaspari, S. Krishnan, G. Cuda, P. Joshi, J.K. Gambhir, S.K. Sharma, A.K. Prasad, L. Saso, R.C. Rastogi, V.S. Parmar, H.G. Raj, Protein acyltransferase function of purified calreticulin: the exclusive role of P-domain in mediating protein acylation utilizing acyloxycoumarins and acetyl CoA as the acyl group donors, Protein Pept. Lett. 18 (2011) 507–517 (Pubmed: 21235489).

[15] F.F. Xu, T.Q. Tao, X.R. Wang, Y.Z. Li, D.D. Song, M. Liu, X.H. Liu, Cytosolic calreticulin inhibits microwave radiation-induced microvascular endothelial cell injury through the integrin-focal adhesion kinase pathway, Microcirculation 21 (2014) 717–729 (Pubmed: 24930861).

[16] M. Rolando, C. Stefani, A. Doye, M.I. Acosta, O. Visvikis, H.G. Yevick, C. Buchrieser, A. Mettouchi, P. Bassereau, E. Lemichez, Contractile actin cables induced by Bacillus anthracis lethal toxin depend on the histone acetylation machinery, Cytoskeleton (Hoboken) 72 (2015) 542–556 (Pubmed: 26403219).

[17] S.C. Kim, R. Sprung, Y. Chen, Y. Xu, H. Ball, J. Pei, T. Cheng, Y. Kho, H. Xiao, L. Xiao, N.V. Grishin, M. White, X.J. Yang, Y. Zhao, Substrate and functional diversity of lysine acetylation revealed by a proteomics survey, Mol. Cell 23 (2006) 607–618 (Pubmed: 16916647).

[18] M. Mann, O.N. Jensen, Proteomic analysis of post-translational modifications, Nat. Biotechnol. 21 (2003) 255–261 (Pubmed: 12610572).

[19] P. Ponnan, A. Kumar, P. Singh, P. Gupta, R. Joshi, M. Gaspari, L. Saso, A.K. Prasad, R.C. Rastogi, V.S. Parmar, H.G. Raj, Comparison of protein acetyltransferase action of CRTAase with the prototypes of HAT, ScientificWorldJournal 2014 (2014) 578956 (Pubmed: 24688408).

[20] C.E. Jessop, T.J. Tavender, R.H. Watkins, J.E. Chambers, N.J. Bulleid, Substrate specificity of the oxidoreductase ERp57 is determined primarily by its interaction with calnexin and calreticulin, J. Biol. Chem. 284 (2009) 2194–2202 (Pubmed: 19054761).

[21] He L, de Val N, Morris CD1, Vora N, Thinnes TC, Kong L, Azadnia P, Sok D, Zhou B, Burton DR, Wilson IA, Nemazee D, Ward AB, Zhu J, Presenting native-like trimeric HIV-1 antigens with self-assembling nanoparticles, Nat. Commun. 7 (2016) 12041. (Pubmed: 27349934).

[22] T.Q. Tao, X.R. Wang, M. Liu, F.F. Xu, X.H. Liu, Myofibrillogenesis regulator-1 attenuated hypoxia/reoxygenation-induced apoptosis by inhibiting the PERK/Nrf2 pathway in neonatal rat cardiomyocytes, Apoptosis 20 (2015) 285–297 (Pubmed: 25542256).

[23] J.H. Tinsley, M.H. Wu, W. Ma, A.C. Taulman, S.Y. Yuan, Activated neutrophils induce hyperpermeability and phosphorylation of adherens junction proteins in coronary venular endothelial cells, J. Biol. Chem. 274 (1999) 24930–24934 (Pubmed: 10455168).

[24] X.H. Guo, Q.B. Huang, B. Chen, S.Y. Wang, F.F. Hou, N. Fu, Mechanism of advanced glycation end products-induced hyperpermeability in endothelial cells, Sheng Li Xue Bao 57 (2005) 205–210 (Pubmed: 15830106).

[25] X. Wang, T. Tao, R. Ding, D. Song, M. Liu, Y. Xie, X. Liu, Kidney protection against ischemia/reperfusion injury by myofibrillogenesis regulator-1, Am. J. Nephrol. 39 (2014) 279–287 (Pubmed: 24714450).

[26] P.P. Lie, D.D. Mruk, K.W. Mok, L. Su, W.M. Lee, C.Y. Cheng, Focal adhesion kinase-Tyr407 and -Tyr397 exhibit antagonistic effects on blood-testis barrier dynamics in

the rat, Proc. Natl. Acad. Sci. U. S. A. 109 (2012) 12562–12567 (Pubmed: 22797892).
[27] A.G. Pakhomov, B.V. Dubovick, I.G. Degtyariov, A.N. Pronkevich, Microwave influence on the isolated heart function: I. Effect of modulation, Bioelectromagnetics 16 (1995) 241–249 (Pubmed: 7488257).
[28] J. Boda-Heggemann, A. Régnier-Vigouroux, W.W. Franke, Beyond vessels: occurrence and regional clustering of vascular endothelial (VE-)cadherin-containing junctions in non-endothelial cells, Cell Tissue Res. 335 (2009) 49–65 (Pubmed: 19002500).
[29] M. Schnoor, A. García Ponce, E. Vadillo, R. Pelayo, J. Rossaint, A. Zarbock, Actin dynamics in the regulation of endothelial barrier functions and neutrophil recruitment during endotoxemia and sepsis, Cell. Mol. Life Sci. 74 (2017) 1985–1997 (Pubmed: 28154894).
[30] M. Puthenedam, P.H. Williams, B.S. Lakshmi, A. Balakrishnan, Modulation of tight junction barrier function by outer membrane proteins of enteropathogenic Escherichia coli: role of F-actin and junctional adhesion molecule-1, Cell Biol. Int. 31 (2007) 836–844 (Pubmed: 17382565).
[31] Y. Riahi, Y. Sin-Malia, G. Cohen, E. Alpert, A. Gruzman, J. Eckel, B. Staels, M. Guichardant, S. Sasson, The natural protective mechanism against hyperglycemia in vascular endothelial cells: roles of the lipid peroxidation product 4-hydroxydodecadienal and peroxisome proliferator-activated receptor delta, Diabetes 59 (2010) 808–818 (Pubmed: 20107107).
[32] L.I. Gold, P. Eggleton, M.T. Sweetwyne, L.B. Van Duyn, M.R. Greives, S.M. Naylor, M. Michalak, J.E. Murphy-Ullrich, Calreticulin: non-endoplasmic reticulum functions in physiology and disease, FASEB J. 24 (2010) 665–683 (Pubmed: 19940256).
[33] J.M. Holaska, B.E. Black, D.C. Love, J.A. Hanover, J. Leszyk, B.M. Paschal, Calreticulin is a receptor for nuclear export, J. Cell Biol. 152 (2001) 127–140 (Pubmed: 11149926).
[34] P. Højrup, P. Roepstorff, G. Houen, Human placental calreticulin characterization of domain structure and post-translational modifications, Eur. J. Biochem. 268 (2001) 2558–2565 (Pubmed: 11322874).
[35] M.A. Pallero, C.A. Elzie, J. Chen, D.F. Mosher, J.E. Murphy-Ullrich, Thrombospondin 1 binding to calreticulin-LRP1 signals resistance to anoikis, FASEB J. 22 (11) (2008) 3968–3979 Nov.
[36] M.C. Viswanathan, A.C. Blice-Baum, W. Schmidt, D.B. Foster, A. Cammarato, Pseudo-acetylation of K326 and K328 of actin disrupts Drosophila melanogaster indirect flight muscle structure and performance, Front. Physiol. 6 (2015) 116 (Pubmed: 25972811).
[37] E.M. Berger, G. Cox, L. Weber, J.S. Kenney, Actin acetylation in Drosophila tissue culture cells, Biochem. Genet. 19 (1981) 321–331 (Pubmed: 6166297).
[38] A. Abe, K. Saeki, T. Yasunaga, T. Wakabayashi, Acetylation at the N-terminus of actin strengthens weak interaction between actin and myosin, Biochem. Biophys. Res. Commun. 268 (2000) 14–19 (Pubmed: 10652204).
[39] P. Singh, P. Ponnan, S. Krishnan, T.K. Tyagi, N. Priya, S. Bansal, D. Scumaci, M. Gaspari, G. Cuda, P. Joshi, J.K. Gambhir, D. Saluja, A.K. Prasad, L. Saso, R.C. Rastogi, V.S. Parmar, H.G. Raj, Protein acyltransferase function of purified calreticulin, part 1: characterization of propionylation of protein utilizing propoxycoumarin as the propionyl group donor, J. Biochem. 147 (2010) 625–632 (Pubmed: 20071373).
[40] S. Jalal, K. Chand, A. Kathuria, P. Singh, N. Priya, B. Gupta, H.G. Raj, S.K. Sharma, Calreticulin transacetylase: a novel enzyme-mediated protein acetylation by acetoxy derivatives of 3-alkyl-4-methylcoumarins, Bioorg. Chem. 40 (2012) 131–136 (Pubmed: 22130072).
[41] Kumari R. Seema, G. Gupta, D. Saluja, A. Kumar, S. Goel, Y.K. Tyagi, R. Gulati, A. Vinocha, K. Muralidhar, B.S. Dwarakanth, R.C. Rastogi, V.S. Parmar, S.A. Patkar, H.G. Raj, Characterization of protein transacetylase from human placenta as a signaling molecule calreticulin using polyphenolic peracetates as the acetyl group donors, Cell Biochem. Biophys. 47 (2007) 53–64 (Pubmed: 22130072).
[42] S. Bansal, P. Ponnan, H.G. Raj, S.T. Weintraub, M. Chopra, R. Kumari, D. Saluja, A. Kumar, T.K. Tyagi, P. Singh, A.K. Prasad, L. Saso, R.C. Rastogi, V.S. Parmar, Autoacetylation of purified calreticulin transacetylase utilizing acetoxycoumarin as the acetyl group donor, Appl. Biochem. Biotechnol. 157 (2009) 285–298 (Pubmed: 18795239).